Precise Positioning of SMA Actuator Using Iterative Control

S. C. Ashley, G. Tchoupo, R. M. Mohr, K. K. Leang[†]
Virginia Commonwealth University, Richmond, VA 23284, USA; [†]kkleang@vcu.edu

Abstract:
In this paper, we study the application of iteration-based control to compensate for positioning error due to hysteresis in a shape memory alloy (SMA) actuator. SMA actuators offer relatively large strain (up to 8%) and high strength-to-weight ratio. These advantages make SMAs attractive for a wide variety of actuator designs such as biomedical tools for minimal invasive surgery and active endoscopes. However, SMA-based actuators exhibit significant hysteresis effect which can lead to loss in positioning precision. To address the hysteresis-caused positioning error, we design and apply an iterative learning control algorithm to control an experimental SMA rotary actuator. We show results that demonstrate the efficacy of the method, e.g., the tracking error reduces to approximately 5% of the total displacement range.

Keywords: shape memory alloy, hysteresis, iterative learning control, Preisach hysteresis model.

1 Introduction

In this paper, we investigate the use of iterative learning control to minimize positioning error caused by hysteresis effect in an experimental shape memory alloy (SMA) actuator. SMA (such as nickel-titanium (NiTi)) is a smart material whereby a change in temperature causes it to deform. An important aspect of SMA is its unique ability to "remember" its shape even after experiencing significant deformation. For instance, at low temperature, SMAs can be deformed (at the martensite phase) and they remain in this state until they are heated (to the austenite phase). This unique behavior can be exploited to create SMA-based actuators (or positioners), and compared to other smart material-based actuators – such as piezos – SMAs offer relatively large strain (up to 8%) and high strength-to-weight ratio (e.g., recovery stress > 500 MPa). These advantages make SMAs attractive for applications such as microrobotics [1] and minimum invasive surgery [2]. However, SMAs also exhibit significant hysteresis behavior and it can lead to loss in positioning precision, subsequently limiting the performance of SMAs.

Control methods to minimize hysteresis in SMAs include feedback and model-based approaches. For example, Ma et al. used a PD controller and a Neural Network (NN) model to reduce the average position error to 7% [3]. Also, the robust control method has been exploited for SMAs, e.g., [4]. On the other hand, by using a model, an input can be found to compensate for hysteresis effect [5]. However, the drawbacks of model-based approaches include lack of robustness and the need to determine model parameters experimentally. In general, feedback and model-based approaches reduce the tracking error to 5 − 10%, e.g., see [3].

Recently, an iterative learning control (ILC) algorithm was developed for piezoelectric actuators [6]. In contrast, this study focuses on applying ILC to SMA. The ILC approach [7, 8] is a repetitive control technique, similar to learning to perform a task, whereby a task is repeated until the performance meets some desired specification – e.g., until the tracking error is acceptably small. One advantage of ILC is that it can be easily implemented with minimal system information. Additionally, it is well suited to repetitive operations such as the back and forth motion for cutting during surgery [2]. Even when the operation is not repetitive, ILC can still be used offline to learn the hysteresis-compensating input, and then the input can be applied to the SMA system – as a feedforward input – to achieve precise positioning. The contribution of this study is to demonstrate the application of an ILC algorithm to compensate for hysteresis in an SMA actuator. We show experimental results to demonstrate the efficacy of the approach.

2 Hysteresis Compensation Using ILC

In this section, we review an ILC method to compensate for hysteresis effect. We begin with a brief description of the Preisach hysteresis model. The model will be used to design an ILC algorithm.

Preisach Hysteresis Model The Preisach model characterizes the hysteresis behavior in smart actuators such as piezo positioners [9] and SMA [10]. In this work we assume the SMA is dominated by hysteresis effect. The Preisach model assumes the output is the net effect of an infinite number of elementary relays R [11]. In this (phenomenological) model, each relay can assume a value of +1 or −1 depending on the applied input. Associated with each relay is a unique pair of "up" and "down" switching values (α, β), such that $\alpha \ge \beta$. The net effect of all the relays produces the output $v(t)$, therefore

$$v(t) = \iint_{\alpha\ge\beta} \mu(\alpha,\beta) R_{\alpha,\beta}[u](t)\, d\alpha\, d\beta \qquad (1)$$

where $\mu(\alpha, \beta)$ is called the Preisach weighting function. We assume each point (α, β) belongs to the restricted Preisach plane **P**, defined as $\mathbf{P} \overset{\Delta}{=} \{(\alpha, \beta) \ge \beta;\ \underline{u} \le \alpha;\ \beta \le \overline{u}\}$. In the α versus β plane, **P** is the limiting upper-right triangle region. In practice, only relays in **P** are affected by the input u.

Depending on which relays have been switched to +1 or −1, at time t the Preisach plane **P** can be divided into two sets, $\mathbf{P}_{\pm}(t) \equiv \{(\alpha, \beta) \in \mathbf{P} : \text{output}(R_{\alpha,\beta}[u](t)) = \pm 1\}$, with $\mathbf{P} = \mathbf{P}_{+}(t) \cup \mathbf{P}_{-}(t)$. The boundary separating the two sets is denoted $L(t)$. Using the relationship $\mathbf{P} = \mathbf{P}_+(t) \cup \mathbf{P}_-(t)$, we can express the output as [10]:

$$v(t) = 2 \iint_{P_+(t)} \mu(\alpha,\beta) d\alpha d\beta - \iint_{P} \mu(\alpha,\beta) d\alpha d\beta \qquad (2)$$

A detailed discussion of the Preisach model can be found in [11].

An ILC Algorithm for SMAs For Preisach-type hysteretic systems, such as SMAs and piezoelectrics, the ILC algorithm (ILCA) of the following form can be used to compensate for hysteresis [6]:

$$u_{k+1}(t) = u_k(t) + \rho[v_d(t) - v_k(t)], \forall t \in [t_i, t_f], \qquad (3)$$

where ρ is a constant (to be determined), and $v_k(t)$ and $u_k(t)$ are the output and input for the k^{th} operating trial, respectively. The ILCA Eq. (3) converges if the desired trajectory v_d is continuous and monotonic over the finite time interval $I = [t_i, t_f]$ [6]. The monotonicity condition is required to overcome the difficulties associated with branching effects in Preisach-type hysteresis behavior. Therefore, if:

1. the weighting function μ is bounded, nonnegative, and piecewise continuous over the Preisach plane **P**, i.e., $0 \le \mu(\alpha, \beta) \le \mu_{max} < \infty$, $\forall (\alpha, \beta) \in \mathbf{P}$, where $\mu_{max} = \max_{\forall(\alpha,\beta)\in P} \mu(\alpha, \beta)$;
2. the initial Preisach state $L(t_i)$ at the initial time t_i (start of the desired output trajectory) is the same for each iteration step k;
3. the desired output $v_d(t)$ is monotonic for all time $t \in [t_i, t_f]$;
4. the initial input $u_0(t)$ is monotonic (and of the same sign in monotonicity as $v_d(t)$) for all time $t \in [t_i, t_f]$;
5. the output-change $(v_2(t) - v_1(t))$ on a branch is bounded above and below by the input difference $(u_2(t) - u_1(t))$ as follows:

$$\eta_1(u_2(t) - u_1(t))^n \le (v_2(t) - v_1(t)) \le \eta_2(u_2(t) - u_1(t)), \qquad (4)$$

   for all time $t \in [t_i, t_f]$, where $\eta_1, \eta_2 > 0$ are constants and n is a positive integer; and
6. the iteration gain ρ is sufficiently small,

then the ILCA converges and the final input u_d (referred to as the desired input) tracks the desired output v_d, i.e., $u_k(t) \to u_d(t)$ as $k \to \infty$ with $v_d(t) = \mathcal{H}[u_d](t)$, for all $t \in [t_i, t_f]$. In particular:

Case 1: when the lower bound on the output change is linear in the input difference ($n = 1$ in Eq. (4)) and the iteration gain ρ satisfies

$$0 < \rho \le \min\left[\frac{1}{\eta_2}, \frac{2}{\eta_1}\right], \qquad (5)$$

then the input sequence generated by the ILCA converges exponentially with the number of iterations k to the desired input u_d, i.e., $\|u_d - u_k\|_\infty \le |1 - \rho\eta|^k \| u_d - u_0\|_\infty$;

Case 2: when the lower bound on the output change is quadratic in the input difference ($n = 2$ in Eq. (4)) and the iteration gain _ satisfies

$$0 < \rho \le \min\left[\frac{1}{\eta_2}, \frac{2}{\eta_1 \Delta u_{\max}}\right], \qquad (6)$$

where Δu_{max} is the maximum input error, then the input sequence generated by the ILCA converges exponentially with the number of iterations k to the desired input ud. That is, $\|u_d - u_k\|_\infty \le |1 - \rho\eta_1\varepsilon|^k \times \||u_d - u_0\|_\infty$, if $\||u_d - u_0\|_\infty > \varepsilon$, where $\varepsilon > 0$ is the acceptable input error and $\| \cdot |_\infty|$ is the maximum value (standard infinity-norm) of a function. Furthermore, the reduction in the output error is exponential with the iteration step k, *i.e.*,

$$\|v_d - v_k\|_\infty \le \begin{cases} \frac{\eta_2}{\eta_1}\left|1 - \rho\eta_1\right|^k \|v_d - v_0\|_\infty, \\ \qquad \text{(if n=1, linear case)} \\ \frac{\eta_2\sqrt{\eta_1}}{\eta_1}\left|1 - \rho\frac{\eta_1}{\eta_2}\varepsilon\right|^k \sqrt{\|v_d - v_0\|_\infty}, \\ \qquad \text{(if n=2, quadratic case)} \end{cases} \qquad (7)$$

where $\varepsilon > 0$ is the acceptable output error. The convergence analysis is described in [6].

Remarks *(i) There always exists a sufficiently small ρ such that convergence is guaranteed (e.g., see Eqs. (5) and (6)); (ii) By Eq. (7) there exists a finite iteration step k* such that the output error reduces to an acceptable level ε > 0.*

The application of ILCA Eq. (3) requires the system to be reinitialized at the start of each iteration, *i.e.*, reinitializing $L(t)$. For convergence, the iteration gain ρ must satisfy Eqs. (5) and (6), and the desired trajectory v_d must be chosen monotonic (single branch). For trajectories v_d with more than one monotonic section (multiple branches), convergence can be achieved by partitioning v_d into the N monotonic sections, and starting with the first, apply the ILCA until a desired tracking precision is achieved. Afterwards, the ILCA is applied to the second section, and then the process is repeated until all N sections have converged to the desired tolerance [6].

3 The Experimental SMA System

To apply the ILCA, a suitable iteration gain ρ is found by modeling the hysteresis behavior. Next, we describe the system and the hysteresis model.

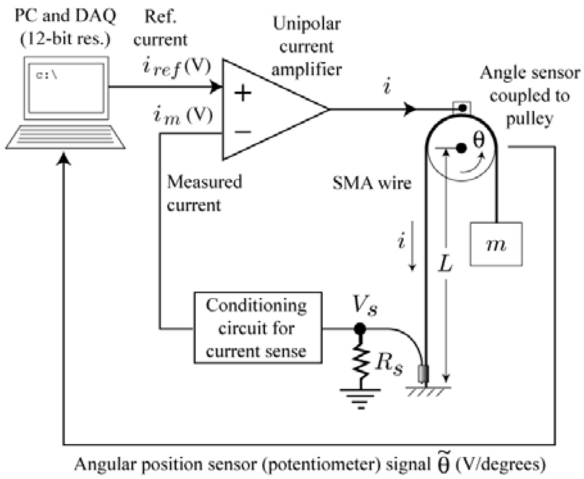

Figure 1: The experimental rotary SMA actuator.

The experimental SMA system is shown in Fig. 1. A one-way Nitinol SMA wire (diameter 100 µm) is fixed at one end and the other end is secured to an aluminum pulley (diameter 2.25 cm), which is free to rotate. An angular position sensor (potentiometer) measures the pulley's angle (gain 22.5°/V). The effective length is L = 22 cm. Rotation is achieved by applying current to heat the wire via the Joule Effect. The heating causes the wire to contract, thus exerting a torque to rotate the pulley. A counter weight (76.05 g) attached to the free end of the wire provides a recovery force to bring the SMA wire (and the pulley's position) to its original state when cooled. The experimental setup was enclosed in a hermetically sealed enclosure to minimize disturbances caused by air currents in the laboratory. A PC equipped with a 12-bit data acquisition card (2.44 mV res.) was used for control and to measure the rotation angle of the SMA actuator. The measurement resolution is 0.055° and the input control resolution is 153 µA; however, a more realistic resolution due to the electrical line-noise of ± 10 mV is 630 µA.

Figure 2(a) shows an open-loop step response for both the heating and the cooling phase. During heating, the 2% settling time was 1.26 s and during cooling, the settling time was 3.49 s. Based on these values, position measurements were acquired after a 10 s period to ensure steady state behavior. The open-loop hysteresis behavior of the SMA actuator is shown in Figs. 2(b)-(d); they show the mismatch between the activation current (i.e., temperature) from martensite to austenite and vice versa. Near the transition zones (~ 80 mA and ~ 120 mA) the output angle θ experience a large change for small changes in the applied current i, i.e., large θ vs. *i* slope. In fact, the maximum slope at the transition is 3.79 °/mA. With the input resolution of 153 − 630 µA, the output can be controlled with resolution 0.58 – 2.39°.

The hysteresis model for the SMA actuator is determined by finding the Preisach weighting function µ. The weighting function µ can be determined from the measured output data using a least-squares approach [12, 13, 6]. Figure 2(e) shows the resulting weighting function µ found by this method. The root-mean-square error between the measured and model output was 0.68° (1.35% of the total 50° range).

4 Experimental Results and Conclusion

Desired Trajectory and Initial Input To illustrate the ILC approach, the desired trajectory $v_d = \theta_d$ was chosen as one monotonically increasing function (in time) as shown in Fig. 2(f) – the actuator rotates from zero to 50°. The initial input current $u_0 = i_0$ is shown in Fig. 2(g). The input is monotonically increasing in time. The input was applied to the SMA system which produced the initial output trajectory θ_0 as shown in Fig. 2(f). The time interval is $T = [t_i, t_f] = [0, 240]$s. Over this time interval, 25 measurements were made. At the start of each iteration, the Preisach state $L(t)$ was reinitialized by cycling the input current between the maximum (189 mA) and minimum (0 mA) values.

Determining the Iteration Gain The iteration gain ρ was determined by finding the constants η_1 and η_2 in the upper and lower bounds on the output difference in Eq. (4)[6]. Using the Preisach weighting function µ and the parameters in the inset shown in Fig. 2(e), $\eta_2 = 2\mu_{max}\Delta u_{max} = 402.19$. For the lower bound, we have two cases: (1) when n = 1, $\eta_1 = 2\sqrt{2}d\mu_{min,band} = 0.013$, and (2) when n = 2, $\eta_1 = \mu_{min,band} = 0.12$. Therefore, the iteration gain ρ based on Eqs. (5) and (6) is $0 < \rho \leq 0.0025$. We note that this value is conservative. In fact, for the initial input i_0 shown in Fig. 2(g), the maximum input change for the first iteration, i.e., $\max(i_1(t) - i_0(t) = \rho(\theta_d(t) - \theta_0(t))$, is 176 µA. This is approximately the input resolution (153 µA). Therefore, we chose the following ρ values to investigate the performance of the ILC control law: ρ = 0.005, 0.010, 0.020.

Tracking Results The ILCA was applied to the SMA actuator and tracking results are shown in Fig. 2(f) - (i). Figures 2(f) and (g) represent the output and input responses, respectively, for ρ = 0.005 and k = 0, 50, 200, 1500. After 1500 iterations, the minimum error is 2.70° (5.4% error over the 50° range). We note that when the input is in the neighborhood of 120 mA (see hysteresis curve in Fig. 2(d)), small changes in the applied current causes relatively large change in the output angle. For example, based on the slope of the hysteresis curve (3.79°/mA), a 153 µA variation can cause the angle to change by 0.58°. The noise level of the system is 10 mV, which equates to 630 µA fluctuation in the input current.

This fluctuation causes 2.39° change in angle, which is approximately the observed minimum tracking error. When ρ = 0.010, tracking error decreases more rapidly (see Fig. 2(h)). After 700 iterations, the minimum tracking error is 3.34°. Finally, for ρ = 0.020, the error converges much faster than the two previous cases; however, the minimum value after 200 iterations is 8.82° (see Fig. 2(i)). Additional iterations did not improve the tracking performance, which suggests that the gain may be too large. In summary, the proposed ILC algorithm compensates for hysteresis provided the iteration gain is sufficiently small, and results showed that performance is limited by the input resolution.

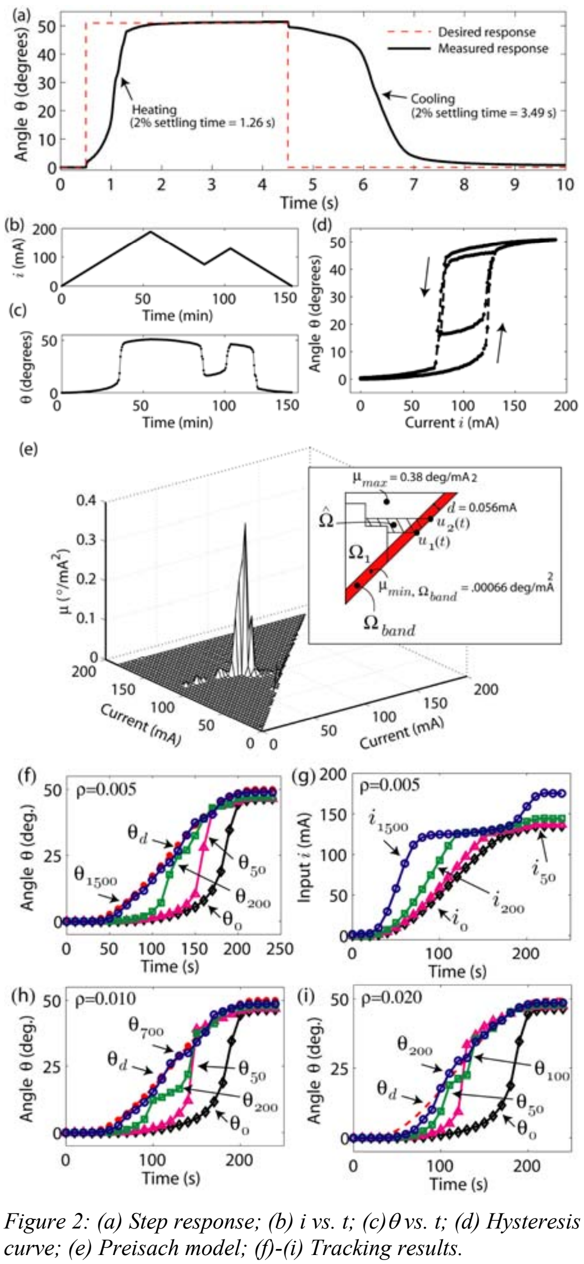

Figure 2: (a) Step response; (b) i vs. t; (c) θ vs. t; (d) Hysteresis curve; (e) Preisach model; (f)-(i) Tracking results.

References

[1] B. Kim, M. G. Lee, Y. P. Lee, Y. Kim, and G. Lee. An earthworm-like micro robot using shape memory alloy actuator. *Sensors and Actuators A*, 125:429 – 437, 2006.

[2] J. M. Stevens and G. D. Buckner. Actuation and control strategies for miniature robotic surgical systems. *ASME Journal of Dynamic Systems, Measurement, and Control*, 127:537 – 549, 2005.

[3] N. Ma, G. Song, and H.-J. Lee. Position control of shape memory alloy actuators with internal electrical resistance feedback using neural networks. *Smart Mater. Struct.*, 13:777–783, 2004.

[4] H. J. Lee and J. J. Lee. Time delay control of a shape memory alloy actuator. *Smart Materials and Structures*, 13:227 – 239, 2004.

[5] L. C. Brinson, A. Bekker, and S. Hwang. Deformation of shape memory alloys due to thermo-induced transformation. *J. Intel. Mater. Syst. Struct.*, 7:97 – 107, 1996.

[6] K. K. Leang and S. Devasia. Design of hysteresis-compensating iterative learning control for piezo positioners: application to atomic force micro-scopes. *Mechatronics*, 6(3-4):141 – 158, 2006.

[7] S. Arimoto, S. Kawamura, and F.Miyazaki. Bettering operation of robots by learning. *J. of Robotic Systems*, 1(2):123–140, 1984.

[8] K. L. Moore, M. Dahleh, and S. P. Bhattacharyya. Iterative learning control: a survey and new results. *J. Robotic Systems*, 9(5):563–594, 1992.

[9] P. Ge and M. Jouaneh. Modeling hysteresis in piezoceramic actuators. *Precision Engineering*, 17(3):211–221, 1995.

[10] R. B. Gorbet, D. W. L Wang, and K. A. Morris. Preisach model identification of a two-wire sma actuator. In *Proc. IEEE Int. Conf. on Robotics and Automation*, pages 2161–2167, 1998.

[11] I. D. Mayergoyz. *Mathematical models of hysteresis*. Springer-Verlag, New York, 1991.

[12] H. T. Banks, A. J. Kurdila, and G. Webb. Identification of hysteretic confluence operators representing smart actuators: convergent approximations. Technical report, North Carolina State University CRSC, April 1997.

[13] W. S. Galinaitis and R. C. Rogers. Control of a hysteretic actuator using inverse hysteresis compensation. In *SPIE Conf. on Mathematics and Control in Smart Structures*, volume 3323, pages 267–277, 1998.